NASA TN D-882

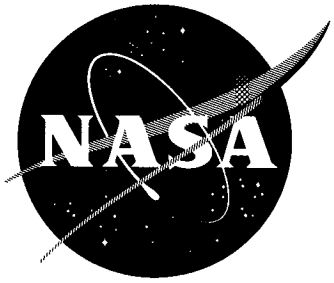

TECHNICAL NOTE

D-882

STRESS CONCENTRATIONS IN FILAMENTARY STRUCTURES

By John M. Hedgepeth

Langley Research Center
Langley Field, Va.

NATIONAL AERONAUTICS AND SPACE ADMINISTRATION
WASHINGTON

May 1961

NATIONAL AERONAUTICS AND SPACE ADMINISTRATION

TECHNICAL NOTE D-882

STRESS CONCENTRATIONS IN FILAMENTARY STRUCTURES

By John M. Hedgepeth

SUMMARY

Theoretical analyses are made of the stress distributions in a sheet of parallel filaments which carry normal loads and are imbedded in a matrix which carries only shear. In all cases, uniform loading at infinity is assumed and small-deflection elasticity theory is used. Static and dynamic stress-concentration factors due to one or more filaments being broken are determined. Particular attention is paid the dynamic overshoot resulting when the filaments are suddenly broken. The dynamic-response factor increases from 1.15 to 1.27 as the number of broken filaments is increased from one to infinity. A somewhat lower dynamic-response factor is obtained when a hole is suddenly caused in the filament sheet.

INTRODUCTION

Structures fabricated from fine filaments that are wound, woven, or plied are becoming prevalent in flight applications. Many solid-propellant rocket-motor cases, for instance, are being constructed by winding resin-coated glass filaments on a mandrel. The high-strength glass filaments carry the pressurization loads and the resin forms a matrix which produces a unitized efficient material. Other applications make use of the good foldability of coated fabrics to package large, low-density structures into small volumes until their erection by mechanical means or inflation is desired.

One of the necessary factors in the rational design of any structure is a knowledge of the behavior of stresses in the neighborhood of discontinuities such as holes and reinforcements. Whereas much information is available about stress concentration in materials which can be considered as continuums, little is known about such stress behavior of filamentary configurations.

Whenever one or more fibers is suddenly broken in a fabric under stress, the load in the broken fiber or fibers must be transferred through the matrix to the adjacent fibers in order to restore equilibrium. Of interest is not only the resulting static stress state but

also the dynamic overshoot which occurs during the transient phase. Both of these results are obtained in this paper for several types of "cutouts" in the simple case of an infinite flat sheet of parallel filaments stressed in uniform tension along the direction of the filaments.

The model treated is that which is common in shear-lag analyses; that is, it is composed of tension-carrying elements connected by purely shear-carrying material. The static problem is solved first and the details of the dynamic analysis are relegated to the appendix. The results are essentially exact within the framework of small-deflection elasticity theory.

SYMBOLS

a,b	major and minor axes of ellipse
d	filament spacing
EA	extensional stiffness of a filament
Gh	shear stiffness of the matrix
K_c	stress-concentration factor for a circular hole
K_e	stress-concentration factor for an elliptical hole
K_r	stress-concentration factor for r broken filaments
L_n	load in nth filament for influence-function solution
m	mass per unit length associated with a filament
n,m	indexes
p	applied force on each filament at infinity
p_n	load in nth filament
P_n	dimensionless load in nth filament
r	number of broken filaments
$R(\ )$	real part of variable

s	Laplace transform variable
t	time
u_n	displacement of nth filament
U	dimensionless displacement
U_n	dimensionless displacement of nth filament
V_n	displacement of nth filament for influence-function solution
x	coordinate parallel to filaments
y	coordinate normal to filaments
z	complex variable
η_c	dynamic-response factor for a circular hole
η_r	dynamic-response factor for r broken filaments
θ	transform variable
ξ	dimensionless coordinate parallel to filaments
σ	dimensionless stress
τ	dimensionless time
φ, ψ	elliptical coordinates

$$\nabla^2 = \frac{\partial(\ )}{\partial x^2} + \frac{\partial(\ )}{\partial y^2}$$

* an asterisk denotes Laplace transform in time

ANALYSIS

The configuration under consideration is shown in figure 1 together with the coordinate and notation systems. The filaments are separated by a constant distance and are numbered from $-\infty$ to ∞ from the bottom upward. The coordinate along the filaments is denoted by x and the

displacement of the nth filament at location x and time t is given by $u_n(x,t)$. Similarly, the force in the nth filament (positive in tension) is called $p_n(x,t)$ and is given in terms of u_n by

$$p_n = EA \frac{\partial u_n}{\partial x} \tag{1}$$

where EA is the extensional stiffness of the filament. The shear force per unit length in the bay between the nth and $(n+1)$st filament is $Gh(u_{n+1} - u_n)/d$ where Gh is the shear stiffness of the matrix. Equilibrium of an element of the nth filament then requires

$$EA \frac{\partial^2 u_n}{\partial x^2} + \frac{Gh}{d}\left(u_{n+1} - 2u_n + u_{n-1}\right) = m \frac{\partial^2 u_n}{\partial t^2} \tag{2}$$

where the assumption has been made that the mass per unit length m associated with the nth filament is concentrated at that filament.

In figure 1, filaments 0 and 1 are shown broken at $x = 0$ and the remainder are shown intact. In general, for r broken filaments, let $0 \leqq n \leqq r - 1$ denote the broken filaments. The appropriate boundary conditions are:

$$\left.\begin{aligned} p_n(0,t) &= 0 \qquad (0 \leqq n \leqq r-1) \\ u_n(0,t) &= 0 \qquad (n < 0 \text{ or } n \geqq r) \end{aligned}\right\} \tag{3}$$

For x large, of course, the force in each filament approaches the uniform applied force which is denoted as p. Thus

$$p_n(\pm\infty,t) = p \tag{4}$$

For the time-dependent problem, the following initial conditions are required:

$$\left.\begin{aligned} p_n(x,0) &= p \\ \frac{\partial u_n}{\partial t}(x,0) &= 0 \end{aligned}\right\} \tag{5}$$

Nondimensionalization

In order to obtain a convenient form for the problem, let

$$\left.\begin{aligned} p_n &= pP_n \\ u_n &= p\sqrt{\frac{d}{EAGh}}\,U_n \\ x &= \sqrt{\frac{EAd}{Gh}}\,\xi \\ t &= \sqrt{\frac{md}{Gh}}\,\tau \end{aligned}\right\} \tag{6}$$

From these equations the following partial-differential—difference equation is obtained:

$$\frac{\partial^2 U_n}{\partial \xi^2} + U_{n+1} - 2U_n + U_{n-1} = \frac{\partial^2 U_n}{\partial \tau^2} \tag{7}$$

with boundary conditions

$$\left.\begin{aligned} U_n(0,\tau) &= 0 \qquad (n < 0 \text{ or } n \geqq r) \\ P_n(0,\tau) &= 0 \qquad (0 \leqq n \leqq r-1) \\ P_n(\pm\infty,\tau) &= 1 \end{aligned}\right\} \tag{8}$$

and initial conditions

$$\left.\begin{aligned} P_n(\xi,0) &= 1 \\ \frac{\partial U_n}{\partial \tau}(\xi,0) &= 0 \end{aligned}\right\} \tag{9}$$

The dimensionless forces and displacements are related by

$$P_n(\xi,\tau) = \frac{\partial U_n}{\partial \xi} \tag{10}$$

Solution of Static Problem

The boundary-value problem for static loading is constituted by equation (7) with the right-hand side set equal to zero and boundary conditions (8). The solution is complicated by the fact that the boundary conditions at $x = 0$ are mixed; that is, they apply to neither U_n nor P_n solely. The following approach is convenient for overcoming this difficulty.

Influence-function technique.- Consider a filament sheet which has no applied edge load and in which all filaments but the zeroeth one are intact. Displace the end of the zeroeth filament a unit amount, maintain zero displacement at $x = 0$ of all the other filaments, and denote the resulting forces and displacements by $L_n(\xi)$ and $V_n(\xi)$. This set of influence functions can then be superposed to obtain the actual problem in the following manner:

$$P_n(\xi) = 1 + \sum_{m=-\infty}^{\infty} L_{n-m}(\xi)\, U_m(0)$$

$$U_n(\xi) = \xi + \sum_{m=-\infty}^{\infty} V_{n-m}(\xi)\, U_m(0)$$

But boundary conditions (8) yield first

$$\left.\begin{aligned} P_n(\xi) &= 1 + \sum_{m=0}^{r-1} L_{n-m}(\xi)\, U_m(0) \\ U_n(\xi) &= \xi + \sum_{m=0}^{r-1} V_{n-m}(\xi)\, U_m(0) \end{aligned}\right\} \qquad (11)$$

since $U_m(0) = 0$ for other values of m, and second

$$0 = 1 + \sum_{m=0}^{r-1} L_{n-m}(0)\, U_m(0) \qquad (0 \leq n \leq r-1) \qquad (12)$$

which is the specification of the boundary conditions on the loads.

Equations (12) constitute a set of r equations for the r unknowns $U_m(0)$. They can be solved and substituted back in equations (11) to yield the entire solution. First, however, the L_n values must be determined.

Determination of the influence functions L_n.- The problem can be stated for $\xi > 0$ as

$$\frac{d^2V_n}{d\xi^2} + V_{n+1} - 2V_n + V_{n-1} = 0 \tag{13}$$

with the conditions

$$\left.\begin{aligned} V_n(0) &= 1 \qquad (n = 0) \\ V_n(0) &= 0 \qquad (n \neq 0) \\ \frac{dV_n}{d\xi}(\infty) &= 0 \end{aligned}\right\} \tag{14}$$

In order to solve this problem, let

$$\overline{V}(\xi,\theta) = \sum_{n=-\infty}^{\infty} V_n(\xi)\, e^{-in\theta} \tag{15}$$

or, inversely,

$$V_n(\xi) = \frac{1}{2\pi} \int_{-\pi}^{\pi} \overline{V}(\xi,\theta)\, e^{in\theta} d\theta \tag{16}$$

Then, multiplying equation (13) by $e^{-in\theta}$ and summing over all n gives

$$\frac{\partial^2\overline{V}}{\partial\xi^2} - 4 \sin^2\frac{\theta}{2}\,\overline{V} = 0 \tag{17}$$

Similar treatment of the boundary conditions (14) yields

$$\left.\begin{aligned} \overline{V}(0,\theta) &= 1 \\ \frac{\partial\overline{V}}{\partial\xi}(\infty,\theta) &= 0 \end{aligned}\right\} \tag{18}$$

The solution satisfying equations (17) and (18) is

$$\overline{V} = e^{-2\left|\sin\frac{\theta}{2}\right|\xi}$$

Thus, from equation (16)

$$V_n(\xi) = \frac{1}{\pi}\int_0^{\pi} \cos n\theta \; e^{-2\xi\sin\frac{\theta}{2}}\, d\theta \tag{19}$$

which can be expressed in terms of Bessel and Weber functions of imaginary argument. For the present purposes, however, the reduction is not necessary since attention will be centered on $L_n(0) = \frac{dV_n}{d\xi}(0)$ which is given simply by

$$L_n(0) = \frac{4}{(4n^2 - 1)\pi} \tag{20}$$

Stress-concentration factors.- Inspection of the problem indicates that the maximum force occurs at $\xi = 0$ in the first intact filament adjacent to the broken ones. Thus, the stress-concentration factor K_r for r broken filaments is given by $P_r(0)$ which equals $P_{-1}(0)$ by virtue of symmetry. Now,

$$P_r(0) = 1 + \sum_{m=0}^{r-1} L_{r-m}(0)\, U_m(0) \tag{21}$$

Solution of equations (12) for the $U_m(0)$ and substitution into equation (21) yields the stress-concentration factor. This process has been carried out for an r of 1 to 6 and the results are given in the following table

r	K_r
1	4/3
2	8/5
3	64/35
4	128/63
5	512/231
6	1,024/429

Inspection of these values show that they can be written as

$$K_r = \frac{4 \cdot 6 \cdot 8 \cdot \cdot \cdot (2r + 2)}{3 \cdot 5 \cdot 7 \cdot \cdot \cdot (2r + 1)} \tag{22}$$

Although this result has not been established in general, its correctness for the first six values lends credence to its validity for all values of r.

Solution of Dynamic Problem

If a Laplace transform is taken of the time-dependent differential equation (eq. (7)) and boundary conditions (eq. (8)), the resulting equations are similar in form to the static equations and the same type of approach can be used for their solution. The details of the solutions are considerably more complicated and are contained in appendix A. The resulting timewise variation of the stress-concentration factor is shown in figure 2 for 1, 2, and 3 broken filaments. Solutions for greater numbers of broken filaments were not obtained because of the increasing difficulty of calculation and because of the existence of an apparent upper limit on the dynamic overshoot. This upper limit is discussed in the next section.

DISCUSSION OF RESULTS

As can be seen from figure 2, the stress-concentration factor exhibits an oscillation that decays in a few cycles to the steady-state value, as the energy is carried away to infinity by wave motion. The oscillations for $r = 1$ and $r = 2$ are fairly simple and are similar to those of a one-degree-of-freedom system. For $r = 3$, the oscillation is more complex, an apparent second-mode component appearing in the time history. In all cases, the first peak is the largest one; the value of the stress at this peak determines the dynamic overshoot and is the principal result to be extracted from the dynamic analysis.

Dynamic-Response Factor

The dynamic-response factor η_r is defined as the ratio between the maximum stress and the static stress. Values for 1, 2, and 3 broken filaments are given in the following table:

r	η_r
1	1.15
2	1.19
3	1.20

The dynamic overshoot thus apparently increases with increasing number of broken filaments. The overshoot can therefore be reasonably expected to be the highest in the limit as the number of broken filaments approaches infinity.

Results for an infinite number of broken filaments.- As has been noted, the greater the number of broken filaments, the greater the difficulty of solution; but the limiting case itself is readily amenable to analysis and is treated in appendix B.

The analysis in appendix B deals with the so-called continuous stringer sheet which is an orthotropic medium with finite extensional stiffness in the longitudinal direction, infinite extensional stiffness in the transverse direction, and finite shear stiffness. Its behavior is governed by the nondimensionalized differential equation

$$\nabla^2 U = \frac{\partial^2 U}{\partial \tau^2} \tag{23}$$

which is obtained either by direct derivation or by replacing the second-order difference in equation (7) with its appropriate derivative equivalent.

The breaking of an infinite number of filaments is accomplished by placing a finite-length slit in the sheet. As is well-known, this procedure leads to an infinite stress-concentration factor in the static problem, the stress varying as the inverse one-half power of the distance from the end of the slit. The stress behaves similarly in the dynamic problem. Thus, the dynamic behavior can be studied by finding the variation of the strength or magnitude of the stress singularity with time. This central result of appendix B is shown in figure 3. As can be seen, the strength C exhibits discontinuities in slope. These discontinuities arise from the reflection of waves issuing from the ends of the slit. Only the first two regimes are shown in figure 3 together with the eventual static value. Results for subsequent regimes are very difficult to obtain and apparently would not contribute any greater stresses. The resulting dynamic-response factor is

$$\eta_\infty = 1.27$$

which should be an upper limit on η_r.

Hole in a stringer sheet.- In the foregoing sections, only slits have been treated. Of interest also is the case in which a hole is punched out of the material. Because of the usefulness of conformal mapping techniques, the static problem is easily analyzed for a large variety of hole shapes for a stringer sheet. In particular, for elliptical shapes, the stress-concentration factor is derived in appendix C to be

$$K_e = 1 + e \tag{24}$$

where e is the ratio between the transverse and longitudinal dimensions of the elliptical hole in the nondimensional coordinate system pertaining to equation (23). For example, a stringer sheet with an elliptical hole that transforms into a circle in the nondimensional coordinate system has a static stress-concentration factor of 2.

In this latter case of a circular boundary, the dynamic problem is also tractable. The analysis is given in appendix C and the variation of K_c with time is shown in figure 4. The resulting dynamic-response factor is

$$\eta_c = 1.08$$

which is considerably less than that for the slit.

CONCLUDING REMARKS

The results derived in this paper lead to the apparent conclusion that the highest dynamic-response factor applicable to the stresses acting in the neighborhood of suddenly induced discontinuities is 1.27. This value was obtained for the case of a long slit in a sheet of closely packed filaments. Either reducing the number of broken filaments or opening the slit into a hole can be expected to decrease the dynamic-response factor.

The analysis was based on elastic, small-deflection theory of a two-dimensional medium. In actuality, filamentary sheets usually have a large number of filaments through the thickness and, whereas the filaments themselves may follow Hooke's law very well, the matrix or the weave introduces large nonlinear effects in the form of plastic deformations, large deflections, and fiber straightening. These factors should act to reduce the stress concentrations and, at least, not increase the dynamic overshoot. In view of the smallness of the dynamic overshoot relative to the possible effects of these other factors, future

theoretical work on this subject would seem to be best devoted to analyzing better models of various types of filamentary construction.

Langley Research Center,
National Aeronautics and Space Administration,
Langley Field, Va., March 20, 1961.

APPENDIX A

DYNAMIC BEHAVIOR OF SHEET WITH SUDDENLY BROKEN FILAMENTS

Let the Laplace transform in time of $U_n(\xi,\tau)$ be denoted by $U_n^*(\xi,s)$ where s is the transform variable. Then, taking transforms of equations (7) and (8) yields

$$\frac{\partial^2 U_n^*}{\partial \xi^2} + U_{n+1}^* - (2 + s^2)U_n^* + U_{n-1}^* = -s\xi \tag{A1}$$

$$\left.\begin{aligned} U_n^*(0,s) &= 0 \qquad (n < 0 \text{ or } n \geqq r) \\ P_n^*(0,s) &= 0 \qquad (0 \leqq n \leqq r-1) \\ \frac{\partial U_n^*}{\partial \xi}(\pm\infty,s) &= \frac{1}{s} \end{aligned}\right\} \tag{A2}$$

where in initial conditions (9) the condition on P_n has been converted to the condition $U_n(\xi,0) = \xi$.

Again, use can be made of the unit solution to write the solution for transformed loads and displacements in the form

$$\left.\begin{aligned} P_n^*(\xi,s) &= \frac{1}{s} + \sum_{m=0}^{r-1} L_{n-m}^*(\xi,s)\, U_m^*(0,s) \\ U_n^*(\xi,s) &= \frac{\xi}{s} + \sum_{m=0}^{r-1} V_{n-m}^*(\xi,s)\, U_m^*(0,s) \end{aligned}\right\} \tag{A3}$$

from which the following equations are obtained

$$0 = \frac{1}{s} + \sum_{m=0}^{r-1} L_{n-m}^*(0,s)\, U_m^*(0,s) \qquad (0 \leqq n \leqq r-1) \tag{A4}$$

and from which the unknown $U_m^*(0,s)$ can be determined. Also, the transformed load in the first intact filament is

$$P_r^*(0,s) = \frac{1}{s} + \sum_{m=0}^{r-1} L_{r-m}^*(0,s)\, U_m^*(0,s) \tag{A5}$$

The transform of the stress-concentration factor K_r^* for r broken filaments is set equal to this transformed load.

As before, $L_n^*(\xi,s) = \frac{\partial V_n^*}{\partial \xi}(\xi,s)$ where $V_n^*(\xi,s)$ satisfies

$$\frac{\partial^2 V_n^*}{\partial \xi^2} + V_{n+1}^* - (2 + s^2)V_n^* + V_{n-1}^* = 0 \tag{A6}$$

and the conditions

$$\left.\begin{aligned} V_n^*(0,s) &= 1 \qquad (n = 0) \\ V_n^*(0,s) &= 0 \qquad (n \neq 0) \\ \frac{\partial V_n^*}{\partial \xi}(\infty,s) &= 0 \end{aligned}\right\} \tag{A7}$$

In order to solve these equations, let

$$\overline{V}^*(\xi,s,\theta) = \sum_{n=-\infty}^{\infty} V_n^*(\xi,s)\, e^{-in\theta} \tag{A8}$$

or, inversely,

$$V_n^*(\xi,s) = \frac{1}{2\pi} \int_{-\pi}^{\pi} \overline{V}^*(\xi,s,\theta)\, e^{in\theta} d\theta \tag{A9}$$

Then equations (A6) and (A7) become, after multiplying by $e^{-in\theta}$ and summing,

$$\left.\begin{aligned} &\frac{\partial^2 \bar{V}^*}{\partial \xi^2} - \left(4 \sin^2 \frac{\theta}{2} + s^2\right)\bar{V}^* = 0 \\ &\bar{V}^*(0,s,\theta) = 1 \\ &\frac{\partial \bar{V}^*}{\partial \xi}(\infty,s,\theta) = 0 \end{aligned}\right\} \tag{A10}$$

The solution for $\xi > 0$ is

$$\bar{V}^* = e^{-\sqrt{4\sin^2 \frac{\theta}{2} + s^2}\ \xi} \tag{A11}$$

which yields

$$V_n^*(\xi,s) = \frac{1}{\pi} \int_0^\pi \cos n\theta\ e^{-\sqrt{4\sin^2 \frac{\theta}{2} + s^2}\ \xi} d\theta \tag{A12}$$

or, finally

$$L_n^*(0,s) = -\frac{1}{\pi} \int_0^\pi \cos n\theta \sqrt{4 \sin^2 \frac{\theta}{2} + s^2}\ d\theta \tag{A13}$$

Solving equations (A4) and substituting into equation (A5) gives the transform of the stress-concentration factor. For 1, 2, and 3 broken stringers, this procedure yields

$$K_1^*(s) = \frac{1}{s}\left(\frac{L_0^* - L_1^*}{L_0^*}\right) \tag{A14a}$$

$$K_2^*(s) = \frac{1}{s}\left(\frac{L_0^* - L_2^*}{L_0^* + L_1^*}\right) \tag{A14b}$$

$$K_3^*(s) = \frac{1}{s}\left[\frac{\left(L_0^* - L_1^*\right)\left(L_0^* - L_3^*\right) - \left(L_1^* - L_2^*\right)^2}{L_0^{*2} + L_0^* L_2^* - 2L_1^{*2}}\right] \tag{A14c}$$

where, for brevity, the functional dependence indicated in equation (A13) is omitted.

The task remains to evaluate $L_n^*(0,s)$ as a function of s and to take the inverse transform of each of equations (A14). This inversion requires integration in the complex s-plane; a study of the behavior of L_n^* (and, therefore, of K_r^*) as functions of the complex variable s is necessary. Such a study shows that L_n^* has branch points at $s = \pm 2i, 0$. (Actually, L_n^* can be written in terms of complete elliptic integrals with modulus

$$k = \left(\sqrt{1 + \frac{s^2}{4}} - \frac{s}{2}\right)^2$$

These elliptic integrals have branch points at $k = \pm 1$. The form of the modulus also guided the choice of conformal mapping used in the sequel.) But the square root in equation (A13) can be thought of as behaving essentially as s for large values of s. Therefore, the branch cuts need not extend to infinity and L_n^* can be made single valued by placing a branch cut along the imaginary axis between $-2i$ and $2i$.

The inversion integral is

$$K_r(\tau) = \frac{1}{2\pi i} \int_{\gamma - i\infty}^{\gamma + i\infty} K_r^*(s) e^{s\tau} ds$$

Since the integrand satisfies Jordan's lemma and the denominators of K_r^* have no zeros except possibly on the branch cut, the integral path can be closed around infinity on the left-hand side and shrunk to the contour C around the branch cut. Thus,

$$K_r(\tau) = \frac{1}{2\pi i} \oint_C K_r^*(s) e^{s\tau} ds \tag{A15}$$

A closed-form evaluation of this integral is probably impossible so that a series evaluation is desirable. One method which is very suitable is as follows:

Let

$$s = z - \frac{1}{z} \tag{A16}$$

This maps the entire s-plane outside the branch cut into the interior of the unit circle. The counterclockwise contour around the branch

cut maps into a clockwise contour just inside the unit circle. Furthermore,

$$L_n^*(0,z) = -\frac{1}{\pi}\int_0^{\pi} \cos n\theta \, \frac{\sqrt{1 - 2z^2\cos\theta + z^4}}{z}\, d\theta$$

which is expandable in a power series in z that is convergent inside the unit circle. Thus,

$$L_n^*(0,z) = -\frac{1}{z}\sum_{k=0}^{\infty}\binom{\frac{1}{2}}{k}\binom{\frac{1}{2}}{k+n}(-z^2)^{2k+n} \qquad \text{(A17)}$$

where

$$\binom{\frac{1}{2}}{k} = \frac{\left(\frac{1}{2}\right)\left(\frac{1}{2} - 1\right)\left(\frac{1}{2} - 2\right)\cdots\left(\frac{1}{2} - k + 1\right)}{k!}$$

is the binomial number.

Making the change of variable gives

$$K_r(\tau) = -\frac{1}{2\pi i}\oint \left[sK_r^*\right]\frac{z^2 + 1}{z^2 - 1}\, e^{\left(z - \frac{1}{z}\right)\tau}\,\frac{dz}{z} \qquad \text{(A18)}$$

The integrand has no singularities within the path of integration except at the origin which is an essential singularity. The value of $K_r(\tau)$ is therefore given simply by the residue of the integrand at $z = 0$. The determination of this residue involves finding the coefficient of the zeroeth power of z in the expansion of

$$\left[sK_r^*\right]\frac{z^2 + 1}{z^2 - 1}\, e^{\left(z - \frac{1}{z}\right)\tau}$$

The series for the bracketed part can be determined from equations (A17) and (A14). It involves only positive even powers of z. So only the negative even powers in the expansion of the other part must be sought. If

$$\frac{z^2 + 1}{z^2 - 1}\, e^{\left(z - \frac{1}{2}\right)\tau} = \sum_{n=-\infty}^{\infty} C_n z^n \qquad \text{(A19)}$$

there results

$$\left.\begin{aligned} C_0 &= -1 \\ C_{-n} &= J_0(2\tau) + 2J_2(2\tau) + \ldots + 2J_{n-2}(2\tau) + J_n(2\tau) - 1 \qquad (n = 2,4,6, \ldots) \end{aligned}\right\} \tag{A20}$$

where J_n is the Bessel function of the first kind.

Proper manipulation and evaluation of the series gives the results plotted in figure 2. Good convergence is obtained and the results are quite accurate.

APPENDIX B

DYNAMIC BEHAVIOR OF A SUDDENLY SLITTED STRINGER SHEET

The required stress distribution can be written

$$\sigma = 1 + \frac{\partial u}{\partial x} \tag{B1}$$

where u satisfies the following dimensionless boundary-value problem

$$\nabla^2 u = \frac{\partial^2 u}{\partial \tau^2} \tag{B2}$$

$$\left.\begin{aligned} u(x,y,0) &= \frac{\partial u}{\partial \tau}(x,y,0) = 0 \\ \frac{\partial u}{\partial x}(0,y,\tau) &= -1 \qquad (-1 < y < 1) \end{aligned}\right\} \tag{B3}$$

Also, u is regular everywhere in the x,y plane except on the slit running from $y = -1$ to $y = 1$ and approaches zero at infinity.

Rather than solve this boundary-value problem directly, the use of an analogy to obtain the stress behavior near the ends of the slit is more convenient. The problem as stated is in exactly the same mathematical form as the problem of determining the perturbation velocity potential in steady supersonic flow (with Mach number of $\sqrt{2}$) over a thin rectangular wing (of span 2) with a very long chord. The time coordinate τ corresponds to the coordinate in the stream direction and the x and y coordinates correspond to the coordinates in the crossflow plane. Zero time is equivalent to the leading edge of the wing which has a constant slope of -1 in the stream direction. Finally, the stresses along the y-axis are the same as the upwash velocities in the tip regions in the plane of the wing.

The existence of this analogy allows the use of the well developed methods of supersonic wing theory; that of Evvard in reference 1 is particularly applicable. This method obtains the upwash velocities in terms of explicit quadratures which are expressible in terms of tabulated functions for the regions close to the leading edge.

The actual detailed analysis by Evvard's method is somewhat tedious and only the resulting formulas of interest are given here. The analysis shows that the stress at the y-axis in the neighborhood of the tip $y = 1$ is of the form

$$\sigma = \frac{C(\tau)}{\sqrt{y - 1}} + O(1) \tag{B4}$$

where $C(\tau)$ is the strength of the singularity and is given by

$$\left.\begin{aligned} C(\tau) &= \frac{2}{\pi}\sqrt{\tau} && (0 < \tau < 2) \\ C(\tau) &= \frac{4}{\pi^2}\left\{\sqrt{\tau + 2}\,(E' - K') + \sqrt{\tau}\left[\frac{\pi}{2}\frac{v}{K} + K'Z(v)\right]\right\} && (2 < \tau < 4) \end{aligned}\right\} \tag{B5}$$

where K and E are complete elliptic integrals of the first and second kind with modulus

$$k = \sqrt{\frac{4}{\tau + 2}}$$

and the primes refer to functions of the comodulus

$$k' = \sqrt{\frac{\tau - 2}{\tau + 2}}$$

The quantity v is determined from the equation

$$\operatorname{sn} v = \sqrt{\frac{\tau + 2}{2\tau}}$$

where $\operatorname{sn} v$ is Jacobi's elliptic sine. Finally, $Z(v)$ is Jacobi's zeta function. (See ref. 2.)

The results are plotted in figure 3. As can be seen, the maximum value of C is reached at $\tau = 2$. The asymptotic value for large τ is obtained from the solution of the static problem:

$$\nabla^2 u = 0$$

$$\frac{\partial u}{\partial x}(0, y, \tau) = -1 \qquad (-1 < y < 1)$$

The solution can be seen to be

$$u(x,y) = R\left(\sqrt{(x + iy)^2 + 1} - x\right)$$

whence the stress is

$$\sigma = R\left(\frac{x + iy}{\sqrt{(x + iy)^2 + 1}}\right)$$

In particular, the stress at the y-axis is

$$\sigma(0,y) = 0 \qquad (|y| < 1)$$

$$\sigma(0,y) = \frac{y}{\sqrt{y^2 - 1}} \qquad (y > 1)$$

so that

$$C(\infty) = \frac{1}{\sqrt{2}}$$

APPENDIX C

STRESS CONCENTRATIONS IN A STRINGER SHEET WITH A HOLE

The stress in an infinite stringer sheet with uniform stress in the x-direction at infinity and with a suddenly induced hole can be written

$$\sigma = \frac{\partial u}{\partial x} \tag{C1}$$

where u satisfies

$$\nabla^2 u = \frac{\partial^2 u}{\partial \tau^2} \tag{C2}$$

and the following initial conditions

$$\left.\begin{aligned} u(x,y,0) &= x \\ \frac{\partial u}{\partial \tau}(x,y,0) &= 0 \end{aligned}\right\} \tag{C3}$$

and boundary conditions

at the boundary of the hole:

$$\frac{\partial u}{\partial n} = 0 \tag{C4a}$$

and at infinity:

$$\frac{\partial u}{\partial x} \to 1 \tag{C4b}$$

These equations are solved in the sequel for two cases: the static stresses around an elliptical hole and the dynamic stresses around a circular hole.

Static Problem

For the first case, let

$$x + iy = c \cosh(\varphi + i\psi)$$

Then the ellipse $\left(\frac{x}{a}\right)^2 + \left(\frac{y}{b}\right)^2 = 1$ maps into $\varphi = \varphi_0$ where

$$c \cosh \varphi_0 = a$$

$$c \sinh \varphi_0 = b$$

The differential equation and boundary conditions become

L
1
5
0
2

$$\frac{\partial^2 u}{\partial \varphi^2} + \frac{\partial^2 u}{\partial \psi^2} = 0 \qquad (\varphi \geqq \varphi_0;\ 0 < \psi < 2\pi)$$

$$\frac{\partial u}{\partial \varphi}(\varphi_0, \psi) = 0 \qquad (0 < \psi < 2\pi)$$

$$u(\varphi, \psi) \sim \frac{c}{2} e^{\varphi} \cos \psi \qquad (\varphi \gg \varphi_0;\ 0 < \psi < 2\pi)$$

This problem has the solution

$$u(\varphi, \psi) = \frac{c}{a - b} (a \cosh \varphi - b \sinh \varphi) \cos \psi$$

Therefore,

$$\sigma = \frac{1}{a - b} \left(a - \frac{b \cosh \varphi \sinh \varphi}{\cosh^2 \varphi - \cos^2 \psi} \right)$$

The maximum stress occurs at $\psi = \frac{\pi}{2}$, $\varphi = \varphi_0$ (at the boundary of the hole on the y-axis) and is

$$\sigma = 1 + \frac{b}{a}$$

As derived, this result is valid only for $a \geqq b$. But a similar derivation for $a \leqq b$ yields the same result. Therefore, the stress concentration factor is

$$K_e = 1 + e \qquad (C5)$$

where e is the ratio of the transverse and longitudinal axes of the ellipse.

Dynamic Problem

For the dynamic problem with a circular hole of unit radius, let

$$\left.\begin{aligned} x &= r\cos\theta \\ y &= r\sin\theta \end{aligned}\right\} \tag{C6}$$

and take the Laplace transform in time. (See appendix A.) The following boundary-value problem results

$$\frac{\partial^2 u^*}{\partial r^2} + \frac{1}{r}\frac{\partial u^*}{\partial r} + \frac{1}{r^2}\frac{\partial^2 u^*}{\partial \theta^2} - s^2 u^* = -sr\cos\theta \tag{C7}$$

$$\left.\begin{aligned} &\frac{\partial u^*}{\partial r}(1,\theta,s) = 0 \\ &u^*(r,\theta,s) \sim \frac{r\cos\theta}{s} \qquad (r \gg 1) \end{aligned}\right\} \tag{C8}$$

The solution is

$$u^*(r,\theta,s) = \frac{\cos\theta}{s}\left[r - \frac{1}{s}\frac{K_1(sr)}{K_1'(s)}\right] \tag{C9}$$

where K_1 is the modified Bessel function of the second kind and the prime denotes differentiation.

The transform of the stress at $x = 0$, $y = 1$ is

$$\sigma^*\left(1,\frac{\pi}{2},s\right) = \frac{1}{s} - \frac{1}{s^2}\frac{K_1(s)}{K_1'(s)} \tag{C10}$$

The stress-concentration factor is given by the inverse transform of equation (C10). Thus,

$$K_c(\tau) = 1 - \frac{1}{2\pi i}\int_{\gamma-i\infty}^{\gamma+i\infty}\frac{K_1(s)}{K_1'(s)}\frac{e^{s\tau}ds}{s^2} \tag{C11}$$

The integrand has a branch point at $s = 0$ and can be made single valued by placing a branch cut along the negative real axis. The

integrand also has two poles located symmetrically in the left-hand half-plane which arise from the zeros of K_1'. By taking account of the residues at these poles, the integration path in equation (C11) can be warped into the path around the branch cut. This latter integral can then be rewritten in real form to yield after some manipulation

$$K_c(\tau) = 2 - \frac{e^{s_0\tau}}{1 + s_0^2} - \frac{e^{\bar{s}_0\tau}}{1 + \bar{s}_0^2}$$

$$+ \int_0^\infty \frac{e^{-\tau\omega}d\omega}{\omega^3\left\{\left[K_0(\omega) + \frac{1}{\omega} K_1(\omega)\right]^2 + \pi^2\left[I_0(\omega) - \frac{1}{\omega} I_1(\omega)\right]^2\right\}} \qquad (C12)$$

where s_0 and $\bar{s}_0$ are the (conjugate) zeros of $K_1'(s)$, and I_0 and I_1 are modified Bessel functions of the first kind.

The value of s_0 was found approximately by interpolation by using the zeros of $K_{1/2}'$, $K_{3/2}'$, and $K_{5/2}'$. The approximate value was then refined by means of the Newton iteration method by using the series expansion for K_1'. The result is

$$s_0 = -0.64355 + 0.50118i$$

The integral in equation (C12) was evaluated numerically after making the substitution

$$\nu = e^{-2\omega}$$

Ten intervals in the range $0 < \nu < 1$ were used together with Simpson's rule.

The results are accurate except for the smallest values of τ. The stress-concentration ratios for these small values were obtained by performing a term-by-term inversion of the asymptotic-series expansion of the right-hand side of equation (C10). The resulting small-time approximation is

$$K_c(\tau) = 1 + \tau - \frac{\tau^2}{4} - \frac{\tau^3}{48} + \ldots \qquad (\tau \ll 1) \qquad (C13)$$

The results are plotted in figure 4.

REFERENCES

1. Evvard, John C.: Use of Source Distributions for Evaluating Theoretical Aerodynamics of Thin Finite Wings at Supersonic Speeds. NACA Rep. 951, 1950.

2. Milne-Thomson, L. M.: Jacobian Elliptic Function Tables. Dover Publications, Inc., 1950.

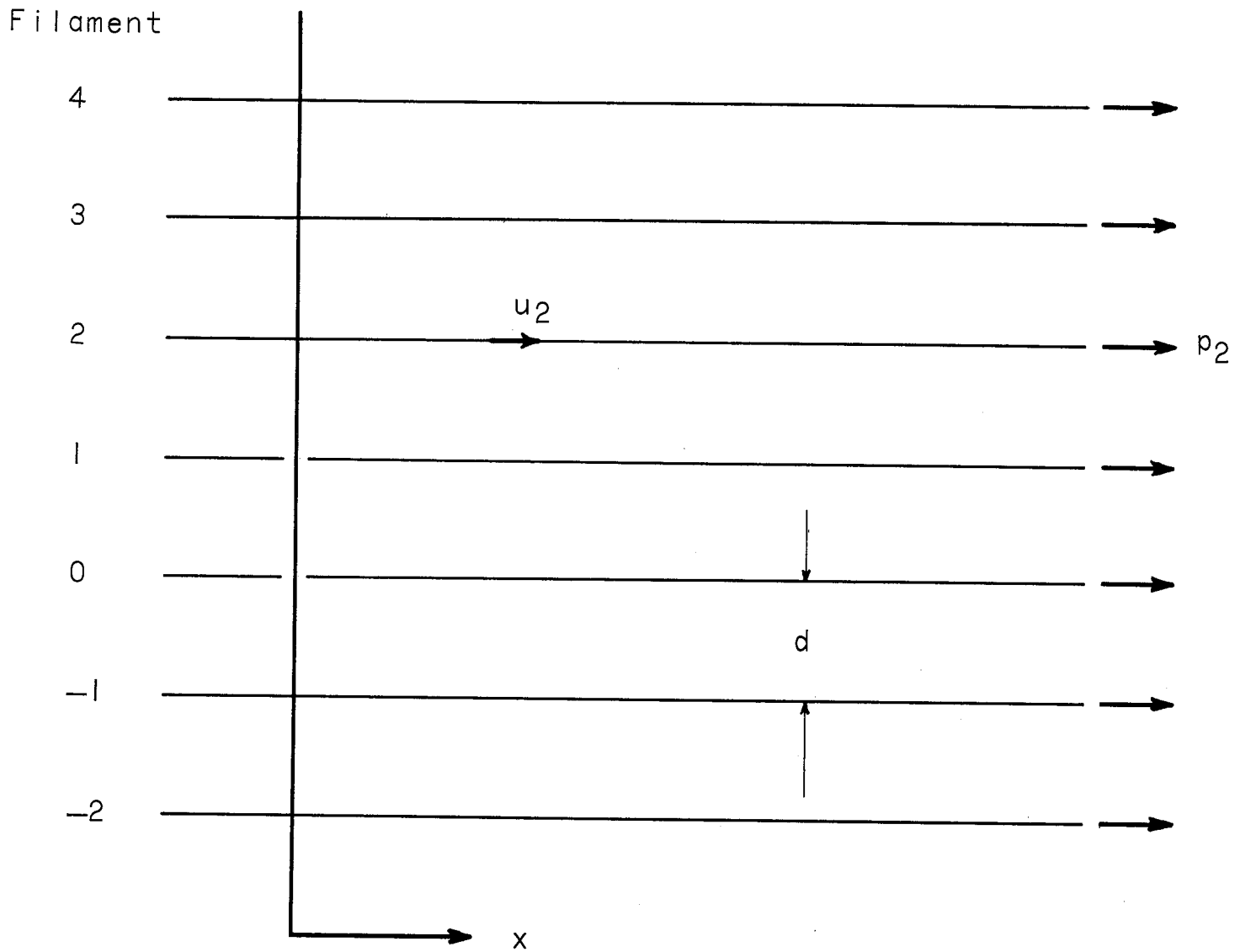

Figure 1.- Coordinate and notation system.

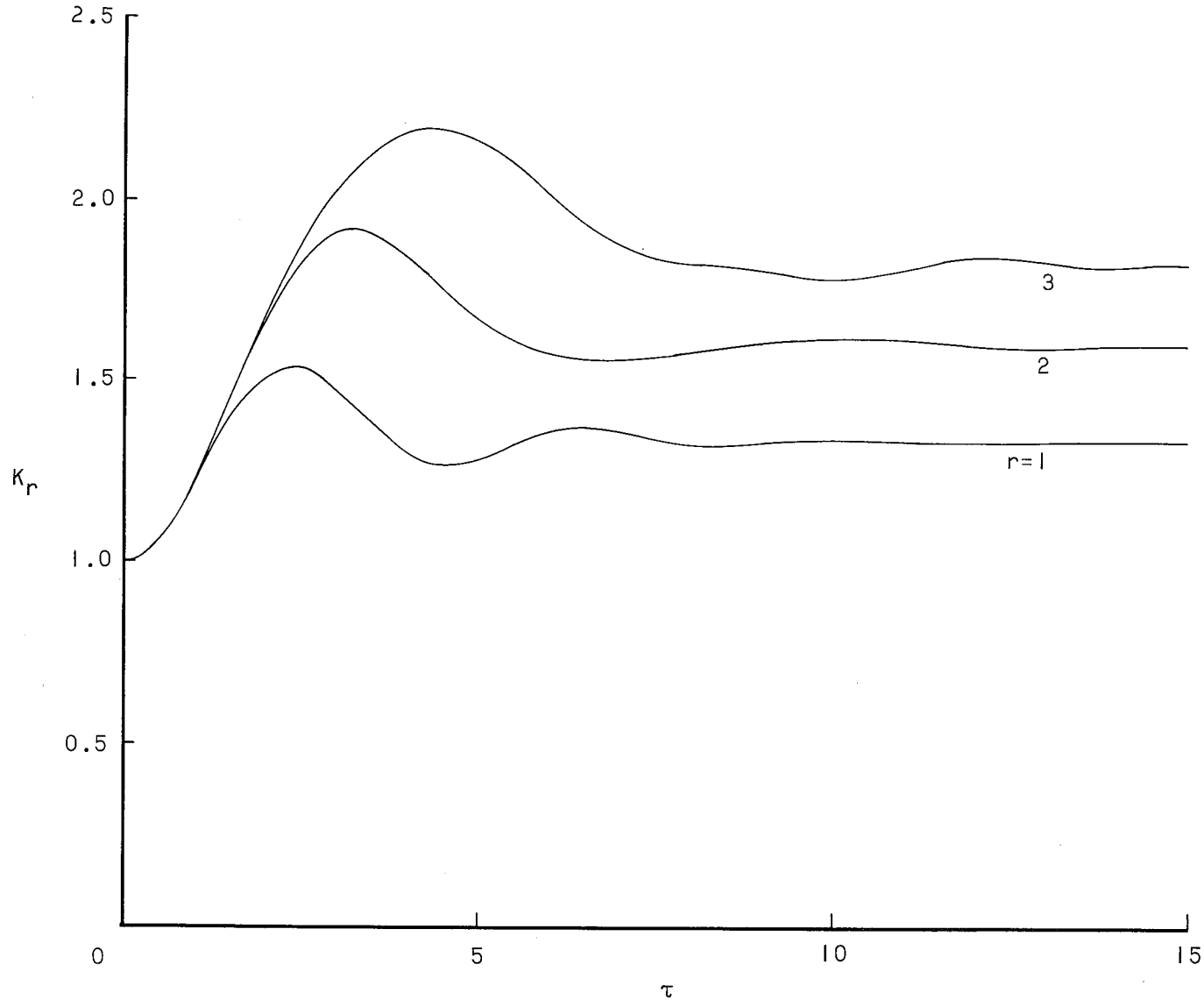

Figure 2.- Variation of stress-concentration factor when r filaments are suddenly broken.

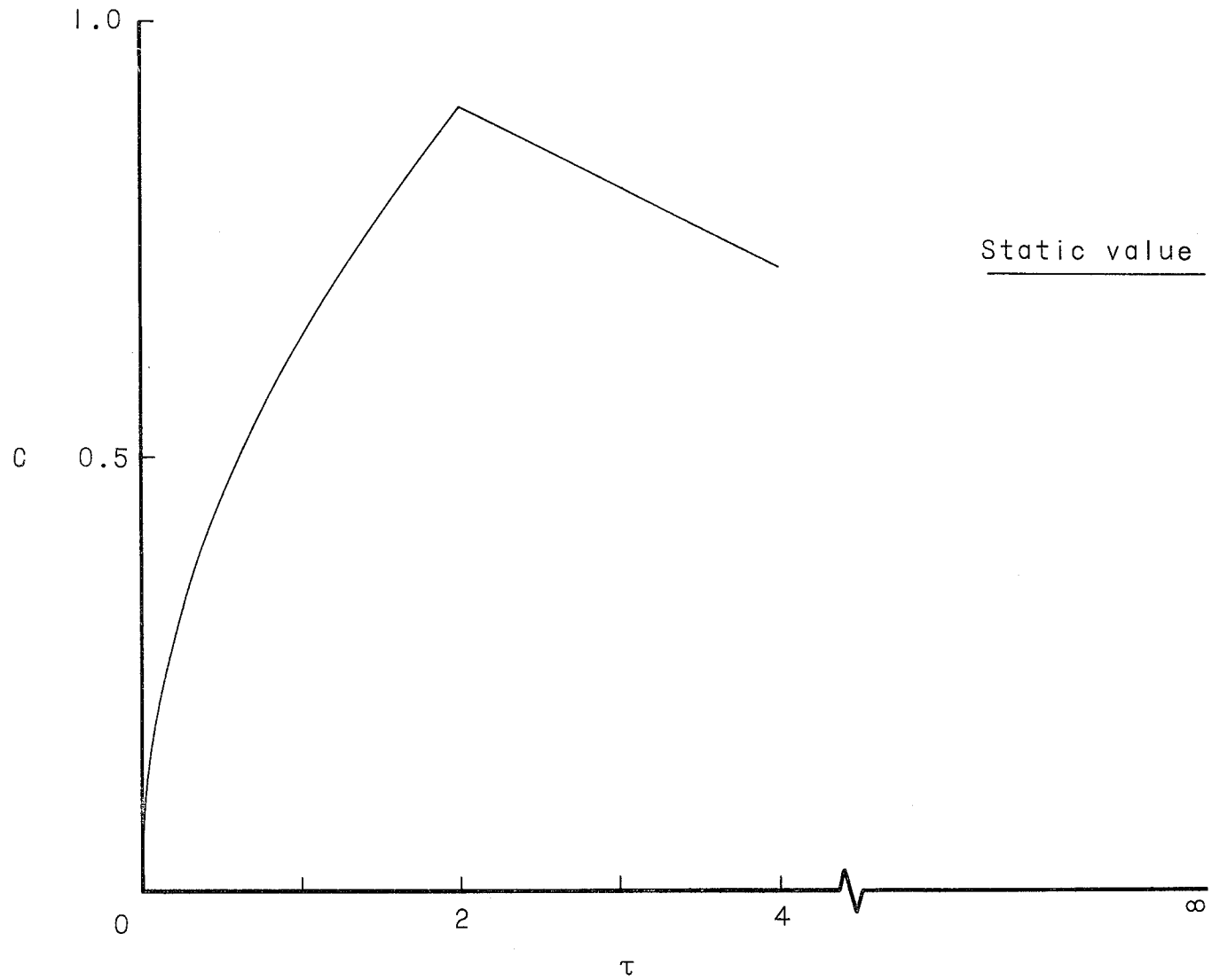

Figure 3.- Variation of the strength of the stress singularity for a stringer sheet in which a slit is suddenly made.

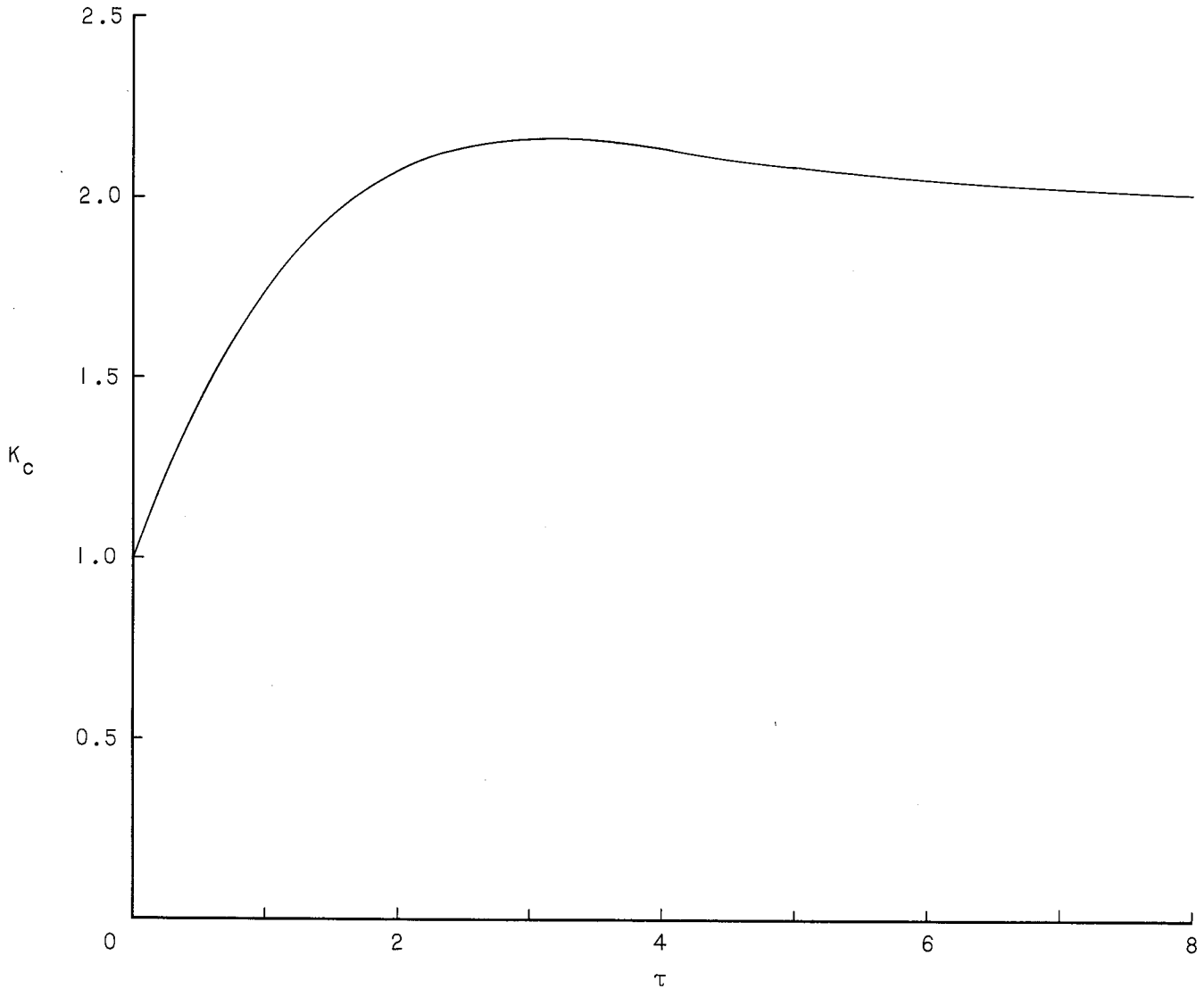

Figure 4.- Variation of the stress-concentration factor for a stringer sheet with a suddenly punched circular hole.

NASA - Langley Field, Va. L-1502

NASA TN D-882
National Aeronautics and Space Administration.
STRESS CONCENTRATIONS IN FILAMENTARY STRUCTURES. John M. Hedgepeth. May 1961.
30p. OTS price, $0.75.
(NASA TECHNICAL NOTE D-882)

Theoretical analyses are made of the stress distributions in a sheet of parallel filaments which carry normal loads and are imbedded in a matrix which carries only shear. In all cases, uniform loading at infinity is assumed and small-deflection elasticity theory is used. Static and dynamic stress-concentration factors due to one or more filaments being broken are determined. Particular attention is paid the dynamic overshoot resulting when the filaments are suddenly broken.

I. Hedgepeth, John Mills
II. NASA TN D-882

(Initial NASA distribution:
51, Stresses and loads;
52, Structures.)

NASA

NASA TN D-882
National Aeronautics and Space Administration.
STRESS CONCENTRATIONS IN FILAMENTARY STRUCTURES. John M. Hedgepeth. May 1961.
30p. OTS price, $0.75.
(NASA TECHNICAL NOTE D-882)

Theoretical analyses are made of the stress distributions in a sheet of parallel filaments which carry normal loads and are imbedded in a matrix which carries only shear. In all cases, uniform loading at infinity is assumed and small-deflection elasticity theory is used. Static and dynamic stress-concentration factors due to one or more filaments being broken are determined. Particular attention is paid the dynamic overshoot resulting when the filaments are suddenly broken.

I. Hedgepeth, John Mills
II. NASA TN D-882

(Initial NASA distribution:
51, Stresses and loads;
52, Structures.)

NASA

NASA TN D-882
National Aeronautics and Space Administration.
STRESS CONCENTRATIONS IN FILAMENTARY STRUCTURES. John M. Hedgepeth. May 1961.
30p. OTS price, $0.75.
(NASA TECHNICAL NOTE D-882)

Theoretical analyses are made of the stress distributions in a sheet of parallel filaments which carry normal loads and are imbedded in a matrix which carries only shear. In all cases, uniform loading at infinity is assumed and small-deflection elasticity theory is used. Static and dynamic stress-concentration factors due to one or more filaments being broken are determined. Particular attention is paid the dynamic overshoot resulting when the filaments are suddenly broken.

I. Hedgepeth, John Mills
II. NASA TN D-882

(Initial NASA distribution:
51, Stresses and loads;
52, Structures.)

NASA

NASA TN D-882
National Aeronautics and Space Administration.
STRESS CONCENTRATIONS IN FILAMENTARY STRUCTURES. John M. Hedgepeth. May 1961.
30p. OTS price, $0.75.
(NASA TECHNICAL NOTE D-882)

Theoretical analyses are made of the stress distributions in a sheet of parallel filaments which carry normal loads and are imbedded in a matrix which carries only shear. In all cases, uniform loading at infinity is assumed and small-deflection elasticity theory is used. Static and dynamic stress-concentration factors due to one or more filaments being broken are determined. Particular attention is paid the dynamic overshoot resulting when the filaments are suddenly broken.

I. Hedgepeth, John Mills
II. NASA TN D-882

(Initial NASA distribution:
51, Stresses and loads;
52, Structures.)

NASA